WITM: Intelligent Traffic Monitoring Using Fine-Grained Wireless Signal

メタデータ	言語: English
	出版者: IEEE
	公開日: 2021-03-09
	キーワード (Ja):
	キーワード (En): Intelligent traffic monitoring, WiFi, CSI, machine learning
	作成者: CHEN, Caijuan, 太田, 香, 董, 冕雄, YU, Chen, JIN, Hai
	メールアドレス:
	所属:
URL	http://hdl.handle.net/10258/00010370

WITM: Intelligent Traffic Monitoring Using Fine-grained Wireless Signal

Caijuan Chen, Kaoru Ota, *Member, IEEE,* Mianxiong Dong, *Member, IEEE,* Chen Yu, *Member, IEEE,* and Hai Jin, *Fellow, IEEE*

Abstract—With the rapid development of the traffic volume, intelligent traffic monitoring technologies have attracted more and more attention, which can support a broad range of applications including traffic congestion mitigation, traffic violation management, and automated driving assistance. Therefore, it is important to realize convenient, effective and intelligent traffic monitoring at low cost. In this paper, we develop a comprehensive traffic monitoring system named WITM, which achieves vehicle detection, vehicle type classification, and vehicle speed estimation by measuring the changes of wireless channel state information. The system shows the advantages of convenient deployment, low cost and easy to expand. The proposed detection processes include three key components, a traffic detection method with moving variance, a CNN-based learning engine to classify the vehicle types, and a combination method of gradient-based and curve fitting to estimate the vehicle speed. By using the fine-grained wireless signal information, WITM achieves vehicle detection with the accuracy of 93.12% and differentiates vehicle types with an accuracy of 87.27%. In addition, the average error of the vehicle speed estimation is less than 5 km/h.

Index Terms—Intelligent Traffic Monitoring, WiFi, CSI, Machine Learning.

I. INTRODUCTION

WITH the substantial growth of urban traffic volume, the traffic condition monitoring has essential significance for traffic safety, urban road planning, and traffic management. Moreover, with the rise of the automatic driving technology and the safety driving assistance system, there are several application requirements for intelligent traffic system (ITS), such as providing necessary traffic information for automated driving systems [1], [2] and detecting pedestrians to improve traffic safety for drivers.

Over the years, a variety of intelligent traffic monitoring technologies are developed to monitor traffic condition. In general, traffic monitoring technologies are based on loop detectors [3], magnetic sensors [4], camera [5], infrared [6], and microwave radar [7], while these existing systems have different disadvantages. The traditional technologies based on the loop detectors or magnetic sensors are intrusive as the ground will be destroyed when the detectors or sensors are buried. Besides, the deployment cost of the inductive loop

C. Chen, C. Yu and H. Jin are with the School of Computer Science and Technology, Huazhong University of Science and Technology. C. Chen was also a visiting student of Muroran Institute of Technology from 2018 to 2019. E-mail: {chencaijuan,yuchen,hjin}@hust.edu.cn

K. Ota, M. Dong are with the Department of Information and Electronic Engineering, Muroran Institute of Technology, Muroran, Hokkaido, Japan. E-mail: {ota, mx.dong}@csse.muroran-it.ac.jp

detectors and sensors is high. Cameras are widely used for traffic monitoring. However, they have the disadvantages of being susceptible to light, weather, and brightness. The non-intrusive technology based on infrared is sensitive to traffic and weather. Detection with the microwave is relatively expensive and generally requires manual control, and the continuous wave Doppler sensor cannot detect the stopped vehicles. Therefore, how to effectively realize traffic monitoring without additional expensive facilities, without interfering with the normal traffic operation, and work well under the dark or bad weather conditions have always been important issues. To overcome these issues, previous studies use wireless sensor network [8], [9], [10] or wireless signals [11], [12] to measure the traffic information. For example, the authors in [11], [12] use the received signal strength (RSS) to monitor the traffic condition.

In recent years, researchers find channel state information (CSI) could provide more detailed wireless information than the classical RSS. Current commercial devices such as Atheros NICs (network interface cards) can obtain these channel information. In recent years, a lot of work has been put forward for action recognition [13], human tracking [14] and state detection [15] based on CSI. The success of these research work and the popularization of wireless networks in traffic monitoring systems [16] inspire us to apply CSI to traffic condition monitoring. However, there are several challenges need to be addressed for traffic information monitoring with CSI. The first challenge is how to extract useful signal information from collected CSI signals to detect the vehicles. It is necessary to detect the actual time segment (start point to finish point) of the vehicles using CSI signals, to estimate the vehicle's type and speed. Furthermore, we need to work out effective methods to measure the traffic information accurately. Another challenge is how to eliminate the interference and noise from other devices or external environment. The raw CSI data contains a lot of irrelevant noise, which makes it impossible to apply the raw CSI values to data analysis directly.

In this paper, we develop an intelligent vehicle monitoring system using WiFi, including the advantages of non-invasive, deploying conveniently, inexpensive, and working well under the darkness. The core theory using CSI for traffic information measurement is that the vehicle will cause interference to the radio signals when the vehicle passes through the wireless link. Because CSI contains more fine-grained information compared with RSS, it becomes a better indicator that measures the signal interference caused by vehicles. At last, we extract
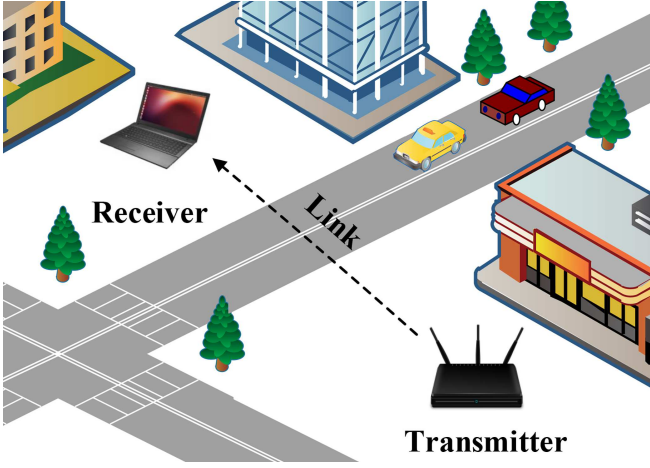
Fig. 1. The experiment layout with a wireless transmitter and a receiver.

traffic information by measuring the changes of CSI. The main contributions of our proposed system are summarized as follows:

- Various signal processing mechanisms are adopted to mitigate the interference of the noise signals. Furthermore, through moving variance, we detect the vehicles' appearance.
- We propose the multi-branch convolutional neural network (CNN) based solution to realize vehicle type classification. The input of CNN is the CSI matrices generated from CSI time series data. In addition, we compare the deep learning method with some traditional machine learning methods.
- A gradient-based approach is developed to find out the start and the finish positions of the signal fragment when the vehicle passes through the wireless link. Then the curve fitting method is used to estimate the vehicle speed.

The rest of the article is organized as follows. First, we discuss the up-to-date studies about traffic monitoring and CSI in Section II. Then, some basic knowledge about CSI is listed in Section III. Next, in Section IV, the overview framework of the traffic monitoring system is illustrated. This is followed by the experimental setup in Section V. After this part, we conduct a real experiment and show the performance of the developed system. Finally, we close this paper with the conclusion in Section VII.

II. RELEATED WORK

A. Traffic Monitoring Technologies

The surveillance of the traffic condition can help us understand the changes and the distribution patterns of the traffic volume in time and space. In addition, it can provide the necessary data support for traffic planning, road construction, traffic management, and engineering economic analysis. Existing traffic monitoring systems adopt a variety of techniques such as inductive loop, computer vision, infrared, etc. The sensors contain two types, which are aggressive and no aggressive sensors. The aggressive sensors mainly include loop detectors [3] and magnetometers [4]. The intrusive sensors have the

advantages of high accuracy but have the flaws of expensive installation, traffic disruption for installation or repair, and high maintenance cost. The non-intrusive sensors such as camera-based sensors [17], microwave radar [7], infrared [6], and ultrasonic [18] sensors are mainly installed above the road or nearby the road. These non-intrusive ones are susceptible to outside environment, including the weather and power hunger.

Mousa et al. [18] combine the passive sound wave sensors and heat sensors to build a novel vehicle monitoring system. The system has the ability to monitor the vehicle velocity, the vehicle numbers, the vehicle density, and the vehicle types. Barcellos et al. [19] use the video camera to achieve traffic detection and count the cars' number. The method based on Gaussian Mixture Models and similarity in adjacent frames is used for vehicle detection and vehicle count. A vehicle classification system is developed in [20] to realize vehicle classification and speed estimation with wireless accelerometers and magnetometers. Adrian et al. [21] focus on the issue of vehicle detection and low power consumption. The authors design, produce and test the vehicle detection module using the magnetic sensors. Al-Tarawneh et al. [22] adopt the SVM algorithm to work out the problem of vehicle classification. They use the grating sensors buried in the pavement to monitor the vehicles' condition. Amal et al. [11] present the RF-based system named Monitor to realize traffic detection and identification, they choose the sliding average and sliding variance techniques to detect moving objects and identify humans or cars with the RSS data. Under the foundation of their work, Kassem et al. [12] develop the RF-based vehicle motion detection and speed estimation system ReVISE to detect vehicles and estimate the vehicle speed.

B. CSI-based Sensing

Most of the previous WiFi-based sensing systems are implemented with RSS, and RSS is widely used for indoor location [23], behavior recognition [24], human-computer interaction [25], etc. Different from RSS, which depicts the superposition effect of multipath propagation, CSI is the physical layer information. Earlier pioneering CSI-based studies mainly focus on human activity recognition such as gesture recognition [26], fall detection [27], human location [14], human identification [28] and environment awareness [29]. Tan et al. [13] propose WiFinger to achieve fine-grained finger gesture recognition. Zheng et al. [30] build the passive smoking system to detect the smoking gesture recognition. WiFall [27] enables to achieve real-time detection of the fall behavior, which is significant for old people living alone. Different from WiFall, Anti-Fall [31] can detect the fall and similar fall actions and identify fall from other similar actions using the signal information. Li et al. [14] present the system MaTrack with the Dynamic-MUSIC method. The developed system can locate the moving human by finding out the angle of the object without any offline training phase. Qian et al. [32] built a system to detect the moving people using the radio signals without any extra devices. The humans can mobile with different velocity values in their experiments. Unlike the previous studies, we apply CSI to intelligent traffic monitoring,

and a system is built to realize vehicle detection, vehicle type classification and vehicle speed estimation.

III. PRELIMINARIES

Popular WiFi standards like IEEE 802.11a/g/n have the ability to support the Orthogonal Frequency Division Multiplex (OFDM). The signal is transmitted through multiple orthogonal subcarriers, and different subcarriers have different amplitude values and phase values. Currently, CSI can provide rich phase and amplitude information of the subcarriers. They describe the comprehensive dynamic changes which include scattering, fading, and power decay of the wireless signal as the places of the wireless devices changes. For each signal captured packet, the data matrices can be presented as

$$H = [H(t_1), H(t_2), \cdots, H(t_m)] \tag{1}$$

where m is the total number of sub-carriers. Notice that channel matrix H can be obtained with the normal NICs and the fine tuned drivers [33], [34].

CSI contains the subcarriers' phase information and amplitude information. A subcarrier's CSI presents a complex value, where we can denote it as

$$H(t_i) = \|(H(t_i))\| e^{j sin\{\angle H(t_i)\}} \tag{2}$$

where $\|(H(t_i))\|$ represents each individual sub-carrier's amplitude, using t_i as the middle frequency of sub-carrier ($i = 1, 2, \cdots, 30$). Besides, $\angle H(t_i)$ represents the phase of the sub-carrier i at the center frequency of t_i.

Then, we give some introduction about the classical Multiple-Input Multiple-Output (MIMO) technology. To improve the data throughput and transmission distances, this technology allows no increment of additional bandwidth and power resource. Generally, multiple antennas are used as transmitters and receivers, where the current standards like 802.11n standard are supported for normal WiFi devices. We use one pair of transmitter and receiver as a stream. Therefore, all the pair of these streams' CSI can be expressed, using $M \times N \times P$. The N and M indicate the number of receivers and transmitters. Besides, the number of sub-carriers is noted as P. A general setting of P is 30, which contains a link from the transmitter to the receiver. As different streams have different propagation paths, the CSI values captured by different streams are various.

Through each received packet, we extract the amplitude and phase data set for one time slot. By analyzing raw phase data captured by the CSI subcarriers, we find that there are no obvious and regular changes of the CSI phase information when the vehicle passes through the wireless devices. The raw phase information of the CSI subcarriers is considered meaningless [32]. In general, most of the vehicles on the road are metal properties, and the impact of metal products on the wireless signal is reflected in the signal amplitude attenuation. Therefore, we use the CSI amplitude information to realize traffic monitoring and discard the phase information.
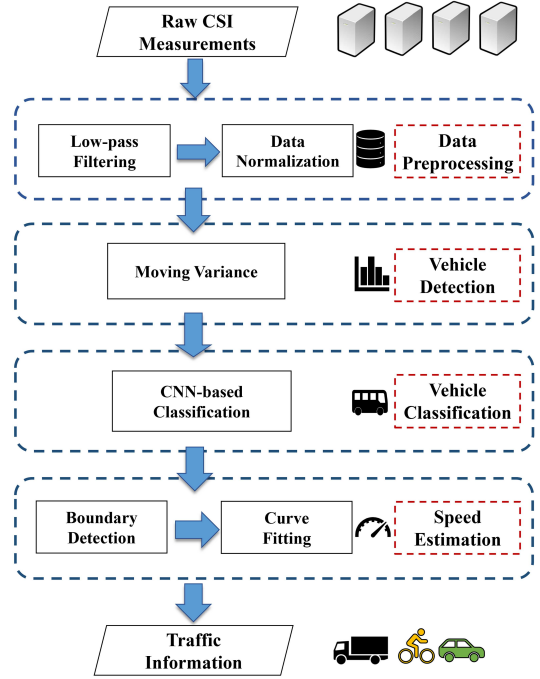

Fig. 2. The architecture overview of WITM, which is composed of data processing, vehicle detection, vehicle classification, and speed estimation.

IV. SYSTEM OVERVIEW

WITM mainly consists of four parts: data preprocessing, vehicle detection with the moving variance method, vehicle classification based on CNN, and vehicle speed estimation using the curve fitting approach. Fig. 2 illustrates the basic structure of the system. First, to get rid of the high frequency signals, the system employs the low-pass filtering. Then, it adopts the normalization approach to eliminate the effect of central frequency diversity. After that, the vehicle is detected by observing the CSI variance changes. If the variance is larger than the predefined threshold, a vehicle is regarded as passing by. After the vehicles are detected, they are used as the input of the multi-branch CNN to train the classification model and achieve the vehicle type identification. At last, for the same type vehicles, the method based on gradient is used to find the start and finish position of the vehicles passing by. The polynomial curve fitting methods which include linear fitting, quadratic fitting, and cubic fitting, are adopted to estimate the vehicle speed.

A. Data Preprocessing

Due to the interference from external environment and hardware devices, such as noise caused by moving people around the wireless devices or the abrupt change of emission intensity of WiFi NICs, the original signal data contains a lot of irrelevant information. Hence, it is inadequate to put the raw CSI data into analysis directly. In this paper, the high frequency waves with noise are removed through the low-pass filter. The data normalization is adopted to solve the problem of the center frequencies diversity.
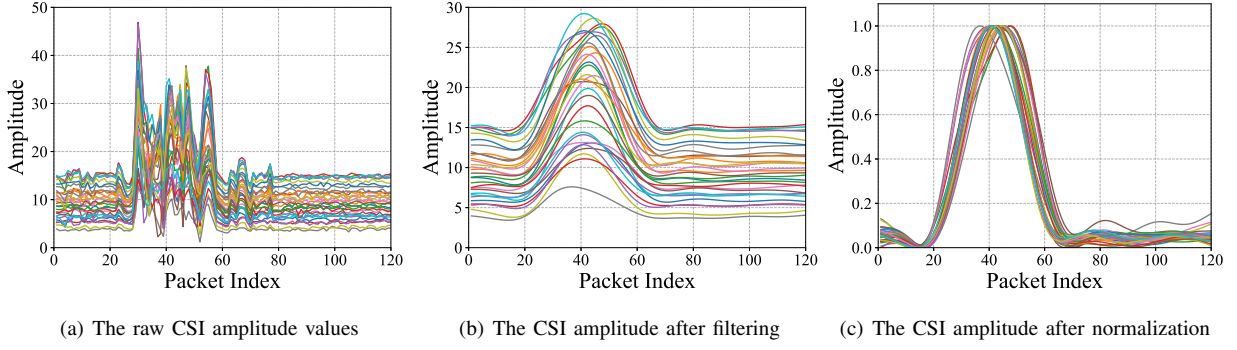
(a) The raw CSI amplitude values   (b) The CSI amplitude after filtering   (c) The CSI amplitude after normalization

Fig. 3. Thirty CSI sequences described with different colors from a pair of transmitting and receiving antennas.

1) Low-pass Filtering: As mentioned in [13], the noise caused by the hardware devices such as the carrier frequency offset and the channel propagation is relatively high frequency. The signal changes introduced by the moving vehicles have a relatively low-frequency. Through low-pass filter, we can get rid of the noise in higher frequency. In Fig. 3(a), it shows the amplitude waveforms of CSI before filtering. Fig. 3(b) demonstrates the result of amplitude waveforms after filtering. We find that the low-pass filter effectively removes the abrupt part of the CSI signals and makes the CSI waveforms formatted.

2) Data Normalization: The center frequencies of different subcarriers are diverse, which result in the diverse ranges of the CSI amplitude, while different CSI waveforms have the same trend under the same condition. To lighten the impact of the different center frequencies on CSI amplitude, we normalize the subcarriers' amplitude separately. For a set of CSI signal data $D = \{d_1, d_2, \cdots, d_m\}$. The data d_{min} is the minimum of among all the values, and d_{max} is the maximum. The normalized data for d_i states $\tilde{d}_i$, which is calculated with the following equation.

$$\tilde{d}_i = \frac{d_i - d_{min}}{d_{max} - d_{min}} \tag{3}$$

Fig. 3(b) is the filtered CSI amplitude waveforms before normalization. In Fig. 3(c), we can observe the CSI waveforms after normalization. We figure out that the trends of the signal amplitude curves are almost consistent after normalization, which illustrates that the data normalization method can eliminate the influence of the diverse CSI signal amplitude ranges caused by the diverse central frequencies.

B. Vehicle Detection

Before measuring the traffic information, we need to segment the continuous sampled CSI signal to find out the time of the vehicle passing by. When the vehicle passes through the transmitter and the receiver, the wireless signal will fluctuate greatly due to the shielding of the vehicle to the wireless signal. As a result, the interference of the vehicle to cause a great influence in the variance of the CSI signal. In our work, the moving variance is able to estimate the time segment of the rushing vehicle. The moving variance method is composed of two steps. First, we slide the CSI time series values into
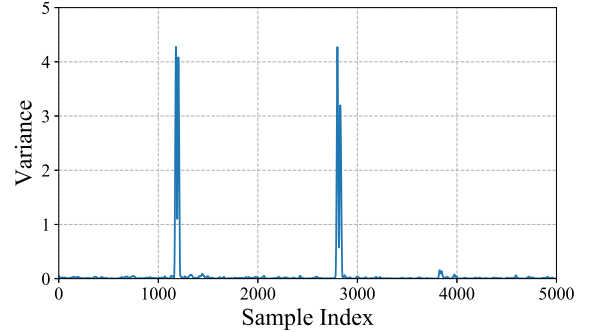

Fig. 4. The CSI amplitude moving variance when the window size is 30.

fixed window sizes with the pre-defined step length. Then, we calculate the variance of CSI data in the windows. The CSI signal sequence can be represented as $D = \{d_1, d_2, \cdots, d_m\}$. The formula of the moving variance can be described as

$$v_i = \frac{\sum_{j=1}^{n}(d_{i+j-1} - \overline{d})^2}{n} \quad and \quad \overline{d} = \sum_{x=i}^{i+n} d_x/n \tag{4}$$

where we use the symbol n to represent the window size of the sliding window. The window size is set to 30 empirically which means every window contains 30 packets from the CSI sequence. The symbol v_i represents the variance of the window. In the experiments, we use the CSI data from a transmitting antenna and three receiving antennas. For each packet, we can obtain a total of 90-dimensional data composed of $1 \times 3 \times 30$. Before computing the variances, we weight the normalized 90-dimensional data to get 1-dimensional data. Then we calculate the variances of the weighted 1-dimensional data. If the calculated variance is bigger than a pre-set threshold, a vehicle is considered as passing by. The variance threshold is determined by the experiments.

In Fig. 4, the x-axis represents the packet index of CSI sample, and y-axis means the calculated variance. We can see that there is a sharp fluctuation in the CSI variance waveform when a vehicle passes by. Therefore, the CSI amplitude variances can be regarded as a clear indicator of the vehicle detection.
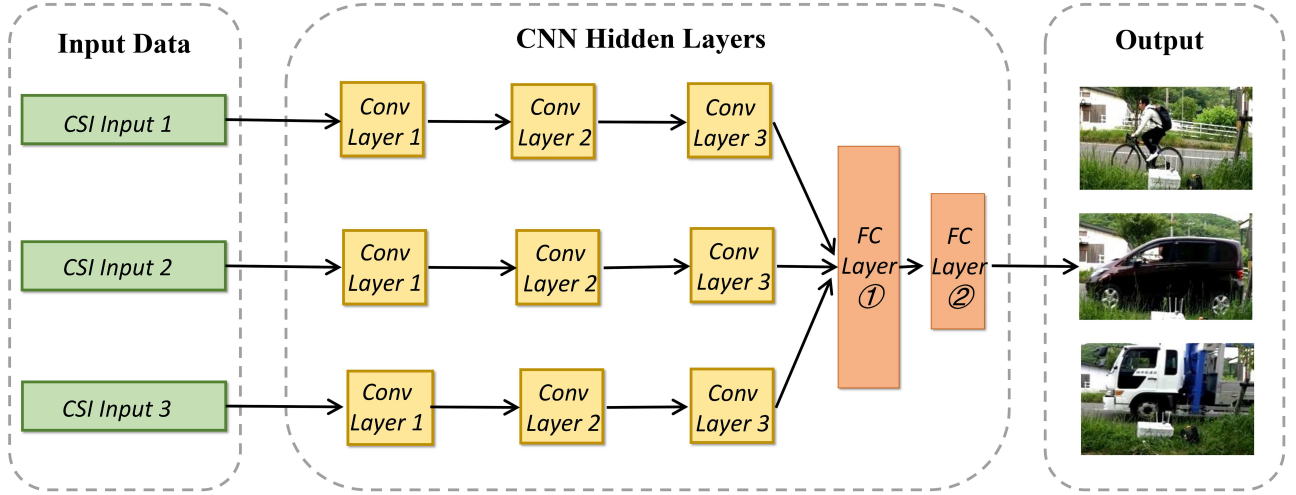
Fig. 5. A convolutional neural network structure for vehicle type classification.

C. Vehicle Type Classification

Due to the size of the vehicles are diverse, the signal changes caused by the vehicles on the wireless signal are different. After the vehicle is detected, we can extract the effective wireless signal information and choose the appropriate approach to judge the vehicle types. Most of the previous researches based on CSI achieve classification using traditional machine learning methods, which require two stages of feature extraction and classification. CNN is a typical deep learning approach, which uses multiple neural cells to generate useful information and achieves classification end-to-end. In view of the successful research work of using CNN to realize location [35], gesture recognition [36] and user authentication [37] based on CSI, we adopt the CNN learning engine to achieve vehicle type classification in this article. Usually, the input of the conventional CNN is the image information. However, when CNN is used to classify the vehicle types in this article, the input is the time series values of the CSI amplitude from different subcarriers. The vehicle types can be classified into three main categories, namely: truck, bus, and two-wheeler.

We can get three streams from one transmitting antenna and three receiving antennas, and every stream can extract 30 CSI subcarriers' values at a time slot. A CSI matrix with the size of $30 \times t$ can be obtained from a stream, and t represents the time segment for the vehicle passing by. We propose a multi-branch CNN structure to solve the vehicle type classification problem. The network framework consists of three branches, and each branch is composed of three convolutional layers. The CSI matrix with the size of $30 \times t$ from a stream as the input of a branch network. The final outputs of the three branches are considered as the input of the full connected layer. In Fig. 5, we give the adopted CNN structure for vehicle type classification. Three branches have the same convolutional layers structure such as the kernel numbers and kernel sizes. The kernel number of the convolutional layer is 6 for the first part, and the kernel size is 30×5. There are 12 different kernels for the second layer and the kernel size of the second layer is still 30×5. After three convolutional layers, 12 feature maps

are generated for each branch network. The kernel size of the last convolutional layer is the same as the second convolutional layer. Then, we concatenate the results of the three branches, so the final outputs of the convolutional layer are 36 feature maps. There are two fully connected layers to achieve the classification. The neuron number of the final fully connected is 3 which is equal to the vehicle types.

The width of the input data for CNN is 30, which is equal to the number of subcarriers. Due to the differences in vehicle sizes and vehicle speeds, the time of the signal fluctuation caused by different vehicles is not consistent. While the input data of the CNN requires the same size, it is a problem to choose the appropriate length of the input map. Because of the limitation of the vehicle speeds and the vehicle sizes, we find that the time of the signal fluctuation caused by the vehicles is less than 1.2 seconds by analyzing the experimental data. We choose the packet delivery rate as 100 packets per second in the tests. Therefore, we set the input data length of the neural network to 120 in this article. As a result, the input of each branch network is a 30×120 matrix. The size of the CSI matrix is still relatively small. We take two measures to ensure that the wireless data information is not lost. On one hand, to keep the size of the map does not change after convolution, the step data of the convolutional layers is one in the network. On the other hand, the sub-sampling layer is not adopted in the neural network structure.

D. Vehicle Speed Estimation

After the vehicle types are judged, we estimate the vehicle speeds of the same type vehicles. The previous work [12] mentions that the vehicle speeds are related to the time length of the signal waveform fluctuation. They use the statistic method and curve fitting method to estimate the vehicle speeds. By analyzing the lengths of fluctuation time of the CSI waveforms, we find that the lengths of time of the signal fluctuation are relevant with the vehicle speeds. In other words, the faster the speed, the less time it will affect the waveform.

In order to get the time length, we need to find out the signal boundary of the signal fluctuation caused by a passing
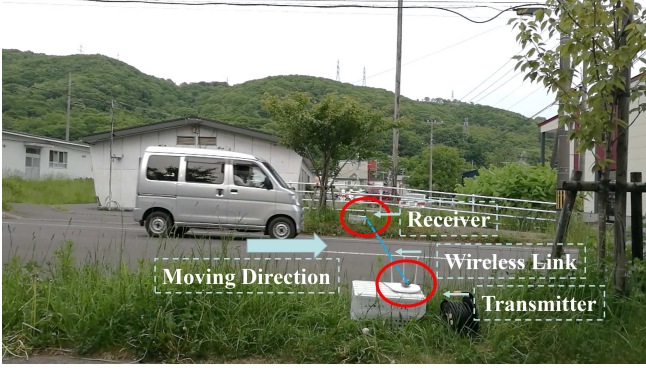
Fig. 6. The real experiment deployment of WITM.

vehicle. We use the gradient-based method to judge the signal boundary in our work. After the vehicle detection module, we can obtain the CSI time series values which contain the start and end points with a fixed length window. The values in a same window can be represented as $D = \{d_1, d_2, \cdots, d_m\}$ after filtering, normalization and weighting preprocessing. For a fixed window, the position of maximum slope change is defined as the start point, and the position of minimum slope change is the end using the gradient-based approach. The methods of calculating the start and end points of the vehicle passing through the transmitter and receiver can be expressed as

$$p_s = max(\frac{d_{x+l} - d_x}{l}) \tag{5}$$

$$p_e = min(\frac{d_{x+l} - d_x}{l}) \tag{6}$$

where p_s and p_e represent the start point and end point, respectively. The values of d_x and d_{x+l} are the CSI data at time x and time $x+l$, respectively. The l value is the step size, and the value of l is determined by the experiment. When we get the start and finish position of the signal boundary, we can get the length of time t that the vehicle affects the CSI signals.

As the amount of the same type vehicles is small, and the distribution range of the vehicle speed values is wide. It is not suitable to use relatively complex models such as the deep neural network to estimate the vehicle speeds. In our work, we use the polynomial curve fitting method to estimate the speed values by fitting the speed V and the length of time t. Polynomial regression is a typical method for fitting continuous values. In our experiments, three degrees are used for the curve fitting: linear, quadratic, and cubic. Three streams can be obtained from one transmitting antenna and three receiving antennas. In order to improve the accuracy of the speed estimation, we build models for each stream and combine the estimated results of different streams. The result of the weighted averaging of three streams as the final estimated speed.

V. SYSTEM IMPLEMENTATION

A. Experimental Setup

We evaluate the performance of the WITM by conducting real experiments with the current WiFi devices, and Fig. 6

shows the experimental environment. We use the Tp-Link WiFi router to send the signal. The laptop equipped with Intel 5300 network interface card is considered as the receiver. The bandwidth of the channel is 20 MHz, and the frequency band is 2.5 GHz. We carry out the experiments with a machine equipped with the Intel Core i7-6700K CPU, 32GB memory and NVIDIA GTX 1080 graphics card. We conduct the data collection on the road for two weeks, and we collect a total of nearly 700 marked vehicle values. The width of the road is 6m. Since the time that the vehicle passes through the wireless devices is relatively short, the packet delivery rate is defined as 100 packets per second. The transmitting device and receiving device are placed on either roadway's side. When collecting data with the WiFi devices, we use the camera to record the traffic conditions so that we can tag the dataset conveniently.

B. Vehicle Speed Calculation

To judge the results of the approaches proposed in this article, we need to tag the dataset. The presence of the vehicles and the vehicle types can be marked by observing the video camera easily. The real speed values can be obtained with the video camera using the method proposed in [38]. The process of vehicle speed calculation contains four steps: (1) we mark two points on the road and record its length L; (2) the frame difference method is used to detect the moving vehicle in the video. The frame difference method is one of the most common approaches for moving object detection and segmentation; (3) the time interval ΔT can be obtained with the frames per second fps and the total frames Δf of the vehicle passing through the two points in the video;

$$\Delta T = \frac{\Delta f}{fps} \tag{7}$$

(4) according to the length L and time interval ΔT, the real vehicle speed V can be calculated using the following formula.

$$V = \frac{L}{\Delta T} \tag{8}$$

VI. PERFORMANCE EVALUATION

A. Evaluation Metrics

First, we discuss the metrics for comparing our proposed system's performance.

- Precision: $\frac{TP}{TP+FP}$, where TP is the true positive, and FP states the false positive. Precision means the average ratio of vehicles estimated by the model that are indeed vehicles.
- Recall: $\frac{TP}{TP+FN}$, where FN represents the false negative, and recall represents the ratio that a real vehicle can be correctly detected.
- F1-score: $\frac{2 \times PR}{P+R}$, where P and R represent precision and recall, respectively. It stands for the average of precision value and recall value.
- Accuracy: $\frac{TP+TN}{TP+FP+TN+FN}$, where TN is the true negative. It is used to highlight the most important standard of our proposed the system can correctly identify each vehicle's type.

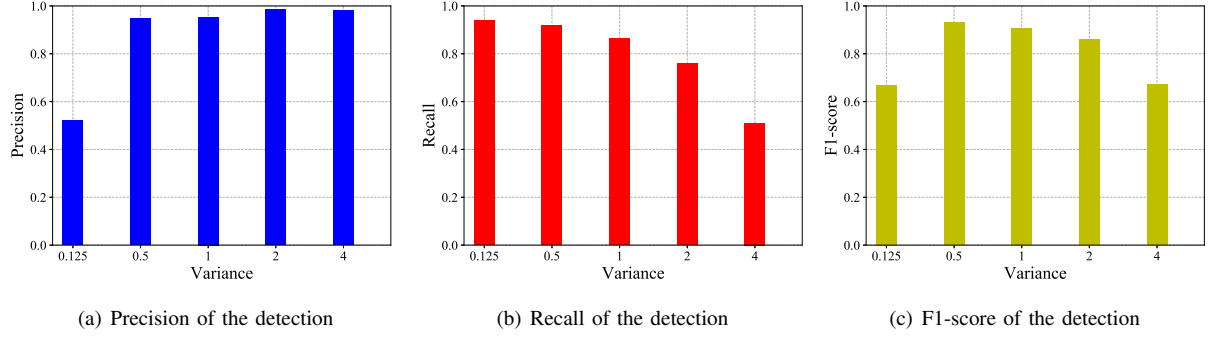(a) Precision of the detection　　　　(b) Recall of the detection　　　　(c) F1-score of the detection

Fig. 7. The results of the vehicle detection experiments when choosing different variances.

- During speed estimation, we use the cumulative probability distribution to present the relative speed error between the estimated speeds and real speeds. The relative velocity error can be calculated with the formula $\frac{|S_t - S_p|}{S_t}$, where S_t is the actual speed, and S_p is the predicted speed.

B. Vehicle Detection

When we choose different variance thresholds, the result of vehicle detection changes. If the threshold is set too high, small fluctuation of the waveforms caused by the vehicles cannot be detected. If the threshold is too small, errors caused by the noise may result in the decrease in the accuracy of the result. Therefore, it is essential to select the appropriate threshold for vehicle detection. Fig. 7(a) and Fig. 7(b) describe the results of precision and recall when we choose different variance thresholds. By analyzing the results, we find that the precision of vehicle detection is relatively higher when the variance increases, which means the rate of a detected vehicle is indeed a vehicle is higher. However, when the variance is set to a large value, the recall becomes smaller. It can be understood that some vehicles cannot be detected when the variance is set to a larger value. Therefore, it is not appropriate to use precision or recall as the evaluation criterion alone.

To emphasize the robustness and accuracy of our proposed system, we use F1-score rather than precision or recall as the final evaluation criteria of the vehicle detection. The results of the F1-score corresponding to different variances, as shown in Fig. 7(c). Through the figure, we know that when the variance value is set to 0.5, the corresponding F1-score can get a larger value of 93.12%. As a result, the variance threshold selected for vehicle detection is 0.5 in this article.

After the variance is determined, we analyze the vehicle detection results as the number of vehicles increases. In Fig. 8(a) and Fig. 8(b), the precision and recall accumulation results increase with the increment of the vehicle numbers. We observe that the precision of vehicle detection is between 95.3% and 96.4%, and the recall of the vehicle detection is between 87.3% and 92%. The experimental results show that the moving variance process is effective enough for vehicle detection.

C. Vehicle Type Classification

We now investigate the performance of vehicle type classification using CNN. Fig. 9 shows the accuracy result of the

(a) The vehicle detection precision with different vehicle numbers　(b) The vehicle detection precision with different vehicle numbers
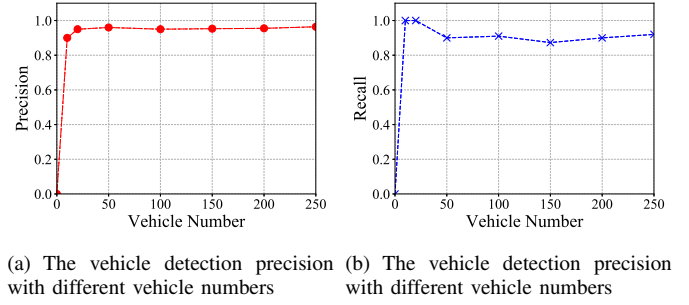
Fig. 8. The vehicle detection results of the experiments when using different vehicle numbers.

CNN classifier with the increment of vehicle numbers. In this experiment, the total train number for CNN is set as 1000 by default. The results demonstrate that the accuracy results of classification are slightly increasing as training set size becomes large. When the training sets' number is 550, the best classification results can be obtained with the accuracy of about 87.3%.

Existed researches based on CSI use the traditional machine learning methods to solve the classification problems such as SVM [39], [40] and KNN [41], [42]. To fully demonstrate the effectiveness of the CNN, we use our proposed method to compare with SVM and KNN. The features adopted in SVM and KNN are listed as follows: (1) root mean square, (2) mean, (3) variance, (4) first quartile, (5) median absolute deviation. Table I shows the average accuracy results of the vehicle type classification for CNN, SVM, KNN with different iteration times. In the experiments, k is set to 5 for KNN because it can achieve the best performance. The results show that the classification accuracy of CNN is consistently better than that of SVM. We find that the accuracy results of CNN are increasing with the iteration numbers increasing. When the iteration number is set to 1000, the accuracy of the classification result of CNN is approximately 87.27%. The classification accuracy results of SVM change with the iteration numbers increasing, and the best classification result is no higher than 77.92%. KNN does not need iteration, so the classification results of KNN don't change with the iteration numbers increasing. The classification accuracy results of KNN are slightly worse than those of SVM and CNN.

TABLE I
THE AVERAGE ACCURACY RATE OF TYPE CLASSIFICATION OF KNN,
SVM, CNN AND WITH THE INCREASE OF THE NUMBER OF ITERATIONS.

Iterations	25	50	100	500	1000
CNN	76.36%	78.18%	81.82%	85.71%	87.27%
SVM	55.09%	74.15%	77.92%	77.64%	77.57%
KNN	–	–	74.53%	–	–
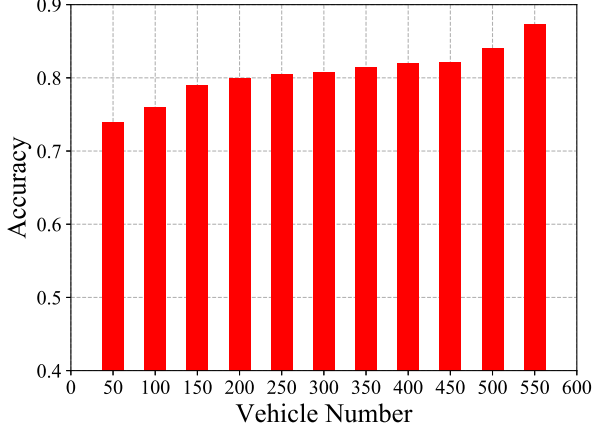
Fig. 9. The accuracy of the vehicle type classification with different vehicle numbers using CNN.

Fig. 10. The cumulative probability distribution of the relative speed error using linear fitting, quadratic fitting and cubic fitting.

D. Vehicle Speed Estimation

When we get the time length of the vehicle passing by with the gradient-based method, the curve fitting method is adopted to estimate the speed for the vehicles of the same type. Three different degrees which include linear, quadratic and cubic are used to fit the speed V and the length of time ΔT for each stream. The final estimated speed is calculated by weighted averaging the results from all streams. In order to compare different polynomial curve fitting methods, the cumulative distribution probability of the relative speed error is applied. Fig. 10 shows the results of the cumulative probability distribution of the relative speed error. The figure demonstrates that the curve fitting using the linear and quadratic performs better than the cubic. The reason for the poor fitting performance of the cubic is overfitting, and the same results can be gotten when the degree increases. We also find that the fitting result of the quadratic is relatively superior, and the corresponding root mean square (RMS) error of vehicle's moving speed is less than 5 km/h with the gradient-based method.

E. Application Evaluation of the System

1) System Latency: The methods proposed in this paper are required to provide timely detection results in some specific scenarios such as the automated driving assistance or the high vehicle velocity. We test the latency time of different modules of the system when the test batch number is 10. The latency for the data preprocessing step is 0.22 seconds which includes the low-pass filtering and data normalization procedures. The time spent 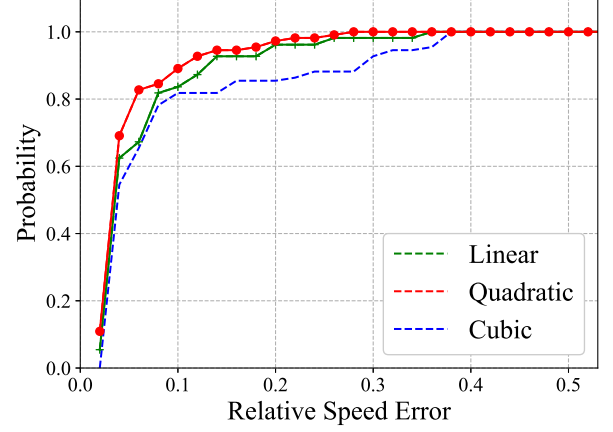on vehicle detection module using moving variance method is 0.06 seconds. The time latency for the test phase of the CNN-based classification module is about 0.07 seconds, and test phase of the speed estimation module costs around 0.01 seconds. The latency values are obtained by averaging the results of 10 runs. The mean total latency time is no more than 0.36 seconds for a batch of 10 vehicles. Therefore, the system can provide timely results and respond quickly to the external environment.

2) System Adaptability: In some countries such as Japan, the statistics of the traffic volume parameters are usually completed by the traffic investigators. Due to the portability and easy deployment of the wireless devices, it is very convenient for the system to replace the investigators to investigate traffic volume parameters under the low traffic condition. In addition, the wireless devices have the advantages of the low price and strong scalability, it is easy to deploy multiple pairs of devices to work together and to extend the system. The system is available for the low traffic scenarios that require large scale deployment devices and low investment such as rural roads. It is also valuable as an auxiliary system when combining with other devices such as cameras or loops.

However, the mechanism of the proposed system is inadequate in the case of the overlapping vehicles. The impact on wireless signals become particularly complicated when multiple vehicles passing by at the same time. Due to the limitations of the current technologies and equipments, more efforts should be made by researchers to effectively separate the superimposed wireless signals to achieve separate detection. Therefore, the proposed method using CSI is designed to get higher accuracy in single-lane or when there is low traffic volume in multiple-lane road.

3) System Potential: In the future research work, we intend to improve the accuracy of the traffic information monitoring under the condition of overlapping vehicles or large traffic volume with a variety of measures such as combining with other sensor devices or mining the internal laws of the wireless signals. Deploying multiple pairs of wireless devices and making full use of wireless signal information such as RSSI, CSI phase information to improve the system stability and

accuracy is also in our plan.

VII. CONCLUSION

In this paper, we develop a system called WITM for intelligent traffic estimation using the fine-grained wireless signal information CSI. First, low-pass filtering is used to process the raw CSI data to remove the interference of the high frequency noise, and data normalization is used to eliminate the diversity of the center frequencies. Then, the moving variance method is presented for vehicle detection. After the vehicle detection, the vehicle type classification is realized using CNN. For the vehicles of the same type, we apply the combination method of gradient-based and curve fitting to vehicle speed estimation process. The results of the experiments show that our developed system can achieve effective traffic monitoring.

ACKNOWLEDGMENT

REFERENCES

[1] C. Zhang, K. Ota, J. Jia, and M. Dong, "Breaking the blockage for big data transmission: Gigabit road communication in autonomous vehicles," *IEEE Communications Magazine*, vol. 56, no. 6, pp. 152–157, June 2018.

[2] L. Li, K. Ota, and M. Dong, "Humanlike driving: Empirical decision-making system for autonomous vehicles," *IEEE Transactions on Vehicular Technology*, vol. 67, no. 8, pp. 6814–6823, Aug 2018.

[3] J. Zhang, S. He, W. Wang, and F. Zhan, "Accuracy analysis of freeway traffic speed estimation based on the integration of cellular probe system and loop detectors," *Journal of Intelligent Transportation Systems*, vol. 19, no. 4, pp. 411–426, 2015.

[4] X. Bao, H. Li, D. Xu, L. Jia, B. Ran, and J. Rong, "Traffic vehicle counting in jam flow conditions using low-cost and energy-efficient wireless magnetic sensors," *Sensors*, vol. 16, no. 11, 2016.

[5] Z. Xu, Y. Liu, L. Mei, C. Hu, and L. Chen, "Semantic based representing and organizing surveillance big data using video structural description technology," *J. Syst. Softw.*, vol. 102, no. C, pp. 217–225, Apr. 2015.

[6] H. Ai and Y. Zheng, "Characterization of a traffic management system using pyroelectric infrared sensors," *Instrumentation Science & Technology*, vol. 43, no. 3, pp. 319–333, 2015.

[7] T. Ho and M. Chung, "An approach to traffic flow detection improvements of non-contact microwave radar detectors," in *2016 International Conference on Applied System Innovation (ICASI)*, May 2016, pp. 1–4.

[8] K. Nellore and G. P. Hancke, "A survey on urban traffic management system using wireless sensor networks," *Sensors*, vol. 16, no. 2, 2016.

[9] W. Balid, H. Tafish, and H. H. Refai, "Development of portable wireless sensor network system for real-time traffic surveillance," in *2015 IEEE 18th International Conference on Intelligent Transportation Systems*, Sept 2015, pp. 1630–1637.

[10] H. Li, K. Ota, M. Dong, and H. Chen, "Efficient energy transport in 60 ghz for wireless industrial sensor networks," *IEEE Wireless Communications*, vol. 24, no. 5, pp. 143–149, October 2017.

[11] A. Al-Husseiny and M. Youssef, "Rf-based traffic detection and identification," in *2012 IEEE Vehicular Technology Conference (VTC Fall)*, Sept 2012, pp. 1–5.

[12] N. Kassem, A. E. Kosba, and M. Youssef, "Rf-based vehicle detection and speed estimation," in *2012 IEEE 75th Vehicular Technology Conference (VTC Spring)*, May 2012, pp. 1–5.

[13] S. Tan and J. Yang, "Wifinger: Leveraging commodity wifi for fine-grained finger gesture recognition," in *Proceedings of the 17th ACM International Symposium on Mobile Ad Hoc Networking and Computing*, ser. MobiHoc '16. New York, NY, USA: ACM, 2016, pp. 201–210.

[14] X. Li, S. Li, D. Zhang, J. Xiong, Y. Wang, and H. Mei, "Dynamic-music: Accurate device-free indoor localization," in *Proceedings of the 2016 ACM International Joint Conference on Pervasive and Ubiquitous Computing*, ser. UbiComp '16. New York, NY, USA: ACM, 2016, pp. 196–207.

[15] K. Ohara, T. Maekawa, and Y. Matsushita, "Detecting state changes of indoor everyday objects using wi-fi channel state information," *Proc. ACM Interact. Mob. Wearable Ubiquitous Technol.*, vol. 1, no. 3, pp. 88:1–88:28, Sep. 2017.

[16] F. Lv, H. Zhu, S. Chang, and M. Dong, "Synthesizing vehicle-to-vehicle communication trace for vanet research," in *2017 IEEE International Conference on Smart Computing (SMARTCOMP)*, May 2017, pp. 1–3.

[17] J. E. Espinosa, S. A. Velastin, and J. W. Branch, "Motorcycle detection and classification in urban scenarios using a model based on faster r-cnn," *CoRR*, vol. abs/1808.02299, 2018.

[18] M. Mousa, E. Oudat, and C. Claudel, "A novel dual traffic/flash flood monitoring system using passive infrared/ultrasonic sensors," in *2015 IEEE 12th International Conference on Mobile Ad Hoc and Sensor Systems*, Oct 2015, pp. 388–397.

[19] P. Barcellos, C. Bouvié, F. L. Escouto, and J. Scharcanski, "A novel video based system for detecting and counting vehicles at user-defined virtual loops," *Expert Syst. Appl.*, vol. 42, pp. 1845–1856, 2015.

[20] W. Ma, D. Xing, A. McKee, R. Bajwa, C. Flores, B. Fuller, and P. Varaiya, "A wireless accelerometer-based automatic vehicle classification prototype system," *IEEE Transactions on Intelligent Transportation Systems*, vol. 15, no. 1, pp. 104–111, Feb 2014.

[21] A. Zarnescu, R. Ungurelu, A. G. Iordache, M. Secere, and M. Spoiala, "Crossroad traffic monitoring using magnetic sensors," in *2017 IEEE 23rd International Symposium for Design and Technology in Electronic Packaging (SIITME)*, Oct 2017, pp. 413–418.

[22] M. Al-Tarawneh, Y. Huang, P. Lu, and D. Tolliver, "Vehicle classification system using in-pavement fiber bragg grating sensors," *IEEE Sensors Journal*, vol. 18, no. 7, pp. 2807–2815, April 2018.

[23] M. Dashti, S. Yiu, S. Yousefi, F. Perez-Cruz, and H. Claussen, "Rssi localization with gaussian processes and tracking," in *2015 IEEE Globecom Workshops (GC Wkshps)*, Dec 2015, pp. 1–6.

[24] B. Mrazovac, B. M. Todorovic, M. Z. Bjelica, and D. Kukolj, "Device-free indoor human presence detection method based on the information entropy of rssi variations," *Electronics Letters*, vol. 49, no. 22, pp. 1386–1388, Oct 2013.

[25] S. Lv, Y. Lu, M. Dong, X. Wang, Y. Dou, and W. Zhuang, "Qualitative action recognition by wireless radio signals in human-machine systems," *IEEE Transactions on Human-Machine Systems*, vol. 47, no. 6, pp. 789–800, Dec 2017.

[26] H. Li, K. Ota, M. Dong, and M. Guo, "Learning human activities through wi-fi channel state information with multiple access points," *IEEE Communications Magazine*, vol. 56, no. 5, pp. 124–129, May 2018.

[27] C. Han, K. Wu, Y. Wang, and L. M. Ni, "Wifall: Device-free fall detection by wireless networks," in *IEEE INFOCOM 2014 - IEEE Conference on Computer Communications*, April 2014, pp. 271–279.

[28] W. Wang, A. X. Liu, and M. Shahzad, "Gait recognition using wifi signals," in *Proceedings of the 2016 ACM International Joint Conference on Pervasive and Ubiquitous Computing*, ser. UbiComp '16. New York, NY, USA: ACM, 2016, pp. 363–373.

[29] X. Zhang, R. Ruby, J. Long, L. Wang, Z. Ming, and K. Wu, "Wihumidity: A novel csi-based humidity measurement system," in *Smart Computing and Communication*, M. Qiu, Ed. Cham: Springer International Publishing, 2017, pp. 537–547.

[30] X. Zheng, J. Wang, L. Shangguan, Z. Zhou, and Y. Liu, "Smokey: Ubiquitous smoking detection with commercial wifi infrastructures," in *IEEE INFOCOM 2016 - The 35th Annual IEEE International Conference on Computer Communications*, April 2016, pp. 1–9.

[31] D. Zhang, H. Wang, Y. Wang, and J. Ma, "Anti-fall: A non-intrusive and real-time fall detector leveraging CSI from commodity wifi devices," *CoRR*, vol. abs/1507.01057, 2015.

[32] K. Qian, C. Wu, Z. Yang, Y. Liu, and Z. Zhou, "Pads: Passive detection of moving targets with dynamic speed using phy layer information," in *2014 20th IEEE International Conference on Parallel and Distributed Systems (ICPADS)*, Dec 2014, pp. 1–8.

[33] Y. Xie, Z. Li, and M. Li, "Precise power delay profiling with commodity wifi," in *Proceedings of the 21st Annual International Conference on Mobile Computing and Networking*, ser. MobiCom '15. New York, NY, USA: ACM, 2015, pp. 53–64.

[34] D. Halperin, W. Hu, A. Sheth, and D. Wetherall, "Tool release: Gathering 802.11n traces with channel state information," *SIGCOMM Comput. Commun. Rev.*, vol. 41, no. 1, pp. 53–53, Jan. 2011.

[35] H. Chen, Y. Zhang, W. Li, X. Tao, and P. Zhang, "Confi: Convolutional neural networks based indoor wi-fi localization using channel state information," *IEEE Access*, vol. 5, pp. 18 066–18 074, 2017.

[36] Y. Ma, G. Zhou, S. Wang, H. Zhao, and W. Jung, "Signfi: Sign language recognition using wifi," *Proc. ACM Interact. Mob. Wearable Ubiquitous Technol.*, vol. 2, no. 1, pp. 23:1–23:21, Mar. 2018.

[37] Q. Wang, H. Li, Z. Chen, D. Zhao, S. Ye, and J. Cai, "Supervised and semi-supervised deep neural networks for csi-based authentication," *CoRR*, vol. abs/1807.09469, 2018.

[38] C. Pornpanomchai and K. Kongkittisan, "Vehicle speed detection system," in *2009 IEEE International Conference on Signal and Image Processing Applications*, Nov 2009, pp. 135–139.

[39] R. Zhou, X. Lu, P. Zhao, and J. Chen, "Device-free presence detection and localization with svm and csi fingerprinting," *IEEE Sensors Journal*, vol. 17, no. 23, pp. 7990–7999, Dec 2017.

[40] W. Yang, X. Wang, A. Song, and S. Mao, "Wi-wheat: Contact-free wheat moisture detection with commodity wifi," in *2018 IEEE International Conference on Communications (ICC)*, May 2018, pp. 1–6.

[41] H. Li, W. Yang, J. Wang, Y. Xu, and L. Huang, "Wifinger: Talk to your smart devices with finger-grained gesture," in *Proceedings of the 2016 ACM International Joint Conference on Pervasive and Ubiquitous Computing*, ser. UbiComp '16. New York, NY, USA: ACM, 2016, pp. 250–261. [Online]. Available: http://doi.acm.org/10.1145/2971648.2971738

[42] Q. Song, S. Guo, X. Liu, and Y. Yang, "Csi amplitude fingerprinting-based nb-iot indoor localization," *IEEE Internet of Things Journal*, vol. 5, no. 3, pp. 1494–1504, June 2018.
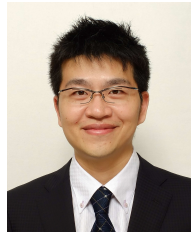
Mianxiong Dong Mianxiong Dong received B.S., M.S. and Ph.D. in Computer Science and Engineering from The University of Aizu, Japan. He is currently a Professor in the Department of Sciences and Informatics, Advisor to Executive Director, and Vice Director of Office of Institutional Research at the Muroran Institute of Technology, Japan. He was a JSPS Research Fellow with School of Computer Science and Engineering, The University of Aizu, Japan and was a visiting scholar with BBCR group at University of Waterloo, Canada supported by JSPS Excellent Young Researcher Overseas Visit Program from April 2010 to August 2011. Dr. Dong was selected as a Foreigner Research Fellow (a total of 3 recipients all over Japan) by NEC C&C Foundation in 2011. He has received best paper awards from IEEE HPCC 2008, IEEE ICESS 2008, ICA3PP 2014, GPC 2015, IEEE DASC 2015, IEEE VTC 2016-Fall, FCST 2017, 2017 IET Communications Premium Award and IEEE ComSoc CSIM Best Conference Paper Award 2018. He has been serving as the Vice Chair of IEEE Communications Society Asia/Pacific Region Information Services Committee and Meetings and Conference Committee, Leading Symposium Chair of IEEE ICC 2019, Student Travel Grants Chair of IEEE GLOBECOM 2019, and Symposium Chair of IEEE GLOBECOM 2016, 2017. He is the recipient of IEEE TCSC Early Career Award 2016, IEEE SCSTC Outstanding Young Researcher Award 2017, The 12th IEEE ComSoc Asia-Pacific Young Researcher Award 2017, Funai Research Award 2018 and NISTEP Researcher 2018 (one of only 11 people in Japan) in recognition of significant contributions in science and technology from MEXT. He is currently the Member of Board of Governors and Chair of Student Fellowship Committee of IEEE Vehicular Technology Society, and Treasurer of IEEE ComSoc Japan Joint Sections Chapter.

Caijuan Chen received the B.S. degree in computer science from Shandong University, Jinan, China, in 2017. Currently, she is pursuing her M.S. degree in Huazhong University of Science and Technology. Her research interests include ubiquitous computing, activity recognition and wireless sensing. She was also a visiting student of Muroran Institute of Technology, during the period of 2018 to 2019.
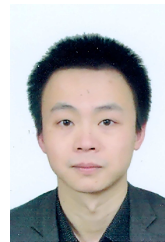
Chen Yu received the B.S. degree in mathematics and the M.S. degree in computer science from Wuhan University, Wuhan, China, in 1998 and 2002, respectively, and the Ph.D. degree in information science from Tohoku University, Sendai, Japan, in 2005. From 2005 to 2006, he was a Japan Science and Technology Agency Postdoctoral Researcher with the Japan Advanced Institute of Science and Technology. In 2006, he was a Japan Society for the Promotion of Science Postdoctoral Fellow with the Japan Advanced Institute of Science and Technology. Since 2008, he has been with the School of Computer Science and Technology, Huazhong University of Science and Technology, Wuhan, where he is currently a full Professor and a Special Research Fellow, working in the areas of wireless sensor networks, ubiquitous computing, and green communications. Dr. Yu was a recipient of the Best Paper Award in the 2005 IEEE International Conference on Communication and the nominated Best Paper Award in the Proceedings of the 11th IEEE International Symposium on Distributed Simulation and Real-Time Application in 2007.

Kaoru Ota was born in Aizu-Wakamatsu, Japan. She received M.S. degree in Computer Science from Oklahoma State University, USA in 2008, B.S. and Ph.D. degrees in Computer Science and Engineering from The University of Aizu, Japan in 2006, 2012, respectively. She is currently an Assistant Professor with Department of Sciences and Informatics, Muroran Institute of Technology, Japan. From March 2010 to March 2011, she was a visiting scholar at University of Waterloo, Canada. Also she was a Japan Society of the Promotion of Science (JSPS) research fellow with Graduate School of Information Sciences at Tohoku University, Japan from April 2012 to April 2013. Her research interests include Wireless Networks, Cloud Computing, and Cyber-physical Systems. Dr. Ota has received best paper awards from ICA3PP 2014, GPC 2015, IEEE DASC 2015, IEEE VTC 2016-Fall, FCST 2017, 2017 IET Communications Premium Award and IEEE ComSoc CSIM Best Conference Paper Award 2018. She is an editor of IEEE Transactions on Vehicular Technology (TVT), IEEE Internet of Things Journal, IEEE Communications Letters, IEEE Wireless Communications Letters, Peer-to-Peer Networking and Applications (Springer), Ad Hoc & Sensor Wireless Networks, International Journal of Embedded Systems (Inderscience) and Smart Technologies for Emergency Response & Disaster Management (IGI Global), as well as a guest editor of ACM Transactions on Multimedia Computing, Communications and Applications (leading), IEEE Internet of Things Journal, IEEE Communications Magazine, IEEE Network, IEEE Wireless Communications, IEEE Access, IEICE Transactions on Information and Systems, and Ad Hoc & Sensor Wireless Networks (Old City Publishing). She is the recipient of IEEE TCSC Early Career Award 2017, and The 13th IEEE ComSoc Asia-Pacific Young Researcher Award 2018.
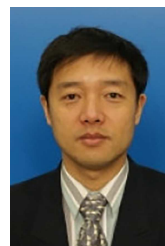
Hai Jin is a Cheung Kung Scholars Chair Professor of computer science and engineering at Huazhong University of Science and Technology (HUST) in China. Jin received his PhD in computer engineering from HUST in 1994. In 1996, he was awarded a German Academic Exchange Service fellowship to visit the Technical University of Chemnitz in Germany. Jin worked at The University of Hong Kong between 1998 and 2000, and as a visiting scholar at the University of Southern California between 1999 and 2000. He was awarded Excellent Youth Award from the National Science Foundation of China in 2001. Jin is the chief scientist of ChinaGrid, the largest grid computing project in China, and the chief scientists of National 973 Basic Research Program Project of Virtualization Technology of Computing System, and Cloud Security. Jin is a senior member of the IEEE and a member of the ACM. He has co-authored 22 books and published over 700 research papers. His research interests include computer architecture, virtualization technology, cluster computing and cloud computing, peer-to-peer computing, network storage, and network security.